Metallomics

RSC Publishing

PAPER

View Article Online
View Journal | View Issue

Cite this: *Metallomics*, 2013, **5**, 920

Effects of metal ions and disulfide bonds on the activity of phosphodiesterase from *Trimeresurus stejnegeri* venom

Lili Peng, Xiaolong Xu,* Mingchun Guo, Xincheng Yan, Shasha Wang, Shang Gao and Shanshan Zhu

Received 28th January 2013,
Accepted 10th June 2013

DOI: 10.1039/c3mt00031a

www.rsc.org/metallomics

Obviously different from the other known phosphodiesterases, the phosphodiesterase from *Trimeresurus stejnegeri* venom (TS-PDE) consists of two different chains linked with disulfide bonds and contains both endogenous Cu^{2+} and Zn^{2+}. Cu^{2+} and Zn^{2+} are important for its phosphodiesterase activity. In this study, the effects of metal ions and small-molecule reductants on its structure and activity have been investigated by polyacrylamide gel electrophoresis, high performance liquid chromatography, fluorescence and electron paramagnetic resonance spectroscopy. The results show that TS-PDE has one class of Zn^{2+} binding site and two classes of Cu^{2+} binding site, including the high affinity activator sites and the low affinity sites. Cu^{2+} ions function as a switch for its phosphodiesterase activity. The catalytic activity of TS-PDE does not have an absolute requirement for Cu^{2+} and Zn^{2+}. Mg^{2+}, Mn^{2+}, Ni^{2+}, Co^{2+} and Ca^{2+} are all effective for its phosphodiesterase activity. TS-PDE has seven disulfide bonds and ten free cysteine residues. L-Ascorbate inhibits the phosphodiesterase activity of TS-PDE through reduction of the Cu^{2+}, while dithiothreitol, glutathione and tris(2-carboxyethyl)phosphine inhibit the phosphodiesterase activity of TS-PDE by reducing both the Cu^{2+} and disulfide bonds. The catalytic activity of TS-PDE relies on its disulfide bonds and bimetallic cluster. In addition, biologically-relevant reductants, glutathione and L-ascorbate, have been found to be endogenous inhibitors to the phosphodiesterase activity of TS-PDE.

Introduction

The phosphodiesterases (PDEs) are a superfamily of enzymes that have multiple roles in nucleotide metabolism and in the regulation of nucleotide-based intercellular signaling.[1,2] PDEs hydrolyze a variety of biologically important nucleotides such as nicotinamide adenine dinucleotide (NAD^+), nicotinamide guanine dinucleotide (NGD), ATP and ADP.[3] PDEs with diverse physiological functions have become new therapeutic targets for treatment of various diseases, such as Alzheimer's disease, inflammation, erectile dysfunction, and cardiac or vascular-related diseases.[1,4–8] Most PDEs are high molecular mass single polypeptide chain proteins with alkaline isoelectric points between 7.5 and 10.5.[3,9,10] Some PDEs exist as homodimers.[11] PDEs are metalloenzymes, most of which contain Zn^{2+}.[12,13] Some PDEs contain Ca^{2+}, Mg^{2+}, Ni^{2+}, Mn^{2+} or Fe^{2+}.[14–16]

Department of Chemistry, University of Science and Technology of China, Hefei, 230026, P. R. China. E-mail: xuxl@ustc.edu.cn; Fax: +86-551-63603388; Tel: +86-551-63603214

Snake venoms are rich in a large variety of proteins and enzymes,[17,18] including PDEs. TS-PDE is a unique PDE isolated from the venom of *Trimeresurus stejnegeri*; among all identified PDEs, only TS-PDE is a disulfide-linked heterodimer with an acidic isoelectric point of 5.1 and contains both endogenous Zn^{2+} and Cu^{2+}.[19] TS-PDE inhibits ADP-induced platelet aggregation and may be useful as a basis for designing anticoagulant drugs to treat thrombosis. Currently, the sequences and structures of all PDEs from snake venoms, including TS-PDE, are not yet available.[3]

In our previous study, we reported that Cu^{2+} and Zn^{2+} are important for the PDE activity of TS-PDE. But it remains unclear whether there is an absolute requirement for Cu^{2+} and Zn^{2+} for the PDE activity of TS-PDE, and whether the valence of the copper ion and the intact disulfide bonds affect the PDE activity of TS-PDE. In the present work, the effects of metal ions and small molecule reductants on the PDE activity and structure of TS-PDE have been investigated. The results indicate that the PDE activity of TS-PDE does not have an absolute requirement for Cu^{2+} and Zn^{2+}. Ca^{2+}, Co^{2+}, Ni^{2+},

Mn^{2+} and Mg^{2+} ions are all activators for its PDE activity. One class of Zn^{2+} binding site and two classes of Cu^{2+} binding site have been identified in the enzyme. The disulfide bonds are essential for the PDE activity of TS-PDE.

Experimental

Chemicals

Lyophilized *Trimeresurus stejnegeri* venom powder was supplied by the Xinyuan Snake Venom Company (Guangzhou, P. R. China). Tris (2-carboxyethyl)phosphine (TCEP), 5,5′-dithiobis-(2-nitrobenzoic acid) (DTNB), glutathione (GSH) and L-ascorbate (Vc) were obtained from Amresco (USA). Dithiothreitol (DTT) was obtained from Merck & Co Inc. (USA). NAD^+ was obtained from Roche (USA). Chelex-100 was purchased from Bio-Rad Laboratories (Richmond, CA, USA). All other reagents were of analytical reagent grade and purchased from Shanghai Chemical Reagent Co. Ltd. (Shanghai, China).

Purification of TS-PDE

The purification of TS-PDE was performed as previously described.[19] Protein purity was confirmed using SDS-PAGE. The concentration of TS-PDE was calculated from the absorption coefficient ($A_{1cm}^{0.1\%}$ = 0.69) at 280 nm and the relative molecular weight (M_r = 100 kDa). Metal-free TS-PDE (apo-TS-PDE) was prepared by incubation of as-purified TS-PDE with a suspension of Chelex-100 in 20 mM Tris-HCl (pH 7.4). Cu^{2+}–Zn^{2+}-TS-PDE (holo-TS-PDE) was prepared by dialysis of apo-TS-PDE extensively against 20 mM Tris-HCl (pH 7.4) containing 5 μM Cu^{2+} and 5 μM Zn^{2+}. Zn^{2+}-reconstituted TS-PDE (Zn^{2+}-TS-PDE) was prepared by dialysis of apo-TS-PDE extensively against 5 μM Zn^{2+} in 20 mM Tris-HCl (pH 7.4). The molar ratios of Cu^{2+} and Zn^{2+} to holo-TS-PDE were determined to be 1.08 ± 0.16 and 0.95 ± 0.12 (mean ± SD, n = 3), respectively, and the molar ratio of Zn^{2+} to Zn^{2+}-TS-PDE was determined to be 2.06 ± 0.19 (mean ± SD, n = 3), and no Cu^{2+} or Zn^{2+} was detected in apo-TS-PDE by inductively coupled plasma-atomic emission spectrometry (ICP-AES) (Perkin Elmer Corporation, USA).

Effect of metal ions on the PDE activity of TS-PDE

0.1 mM NAD^+ was incubated with 2 μM holo-TS-PDE or apo-TS-PDE in 20 mM Tris-HCl (pH 7.4) in the presence of 1 mM Zn^{2+}, Cu^{2+}, Mg^{2+}, Mn^{2+}, Ni^{2+}, Co^{2+} or Ca^{2+} at 37 °C for 15 min. All products were analyzed by an 1100-dHPLC Instrument (Agilent, USA) with a SymmetryShield RP18 column (4.6 × 250 mm) (Waters, USA) at 260 nm. The mobile phase contained 10 mM ammonium phosphate (pH 5.5) and acetonitrile (100 : 1.2 v/v).

0.1 mM NAD^+ was incubated with 2 μM apo-TS-PDE in 20 mM Tris-HCl (pH 7.4) with increasing concentrations of Zn^{2+} or Cu^{2+} at 37 °C for 15 min. The products were analyzed by HPLC. The PDE activity of holo-TS-PDE was taken as 100%.

Fluorescence titration of apo-TS-PDE with Cu^{2+} and Zn^{2+}

For titration of apo-TS-PDE with Cu^{2+} and Zn^{2+}, the metal ion solutions at an appropriate concentration were added serially to 2 μM apo-TS-PDE in 20 mM Tris-HCl (pH 7.4), respectively, in small aliquots following the method of Kumar and Duff.[20] All fluorescence measurements were performed using a Shimadzu RF-5000 spectrofluorometer using an excitation wavelength of 295 nm at 25 °C. The excitation and emission bandwidths were both set at 5 nm. All spectra were corrected by subtracting the spectrum of the blank, lacking the protein but otherwise identical to the sample. All titrations were performed three times. Data were fitted by a modified Stern–Volmer equation.[21] The fraction of the fluorescence that is accessible to the quencher, f_a, and the Stern–Volmer quenching constant (K) that represents the apparent association constant between the fluorophore and quencher[22] can be determined graphically by the following eqn (1):

$$F_0/(F_0 - F) = 1/(f_a K X) + 1/f_a \quad (1)$$

where F_0 and F are the respective fluorescence intensities in the absence and presence of quencher (metal ion), and X is the concentration of the metal ion. A plot of $F_0/(F_0 - F)$ *vs.* $1/X$ yields f_a^{-1} as the intercept on the y-axis and $(f_a K)^{-1}$ as the slope.

Reduction of Cu^{2+} in as-purified TS-PDE by small-molecule reductants

10 μM as-purified TS-PDE was incubated with 25 mM DTT, 15 mM GSH, 10 mM TCEP or 20 mM Vc in 20 mM Tris-HCl (pH 7.4) containing 0.15 M NaCl at 37 °C for 60 min. The absorbance spectrum (400–800 nm) of the mixture was recorded after addition of 1 mM bicinchoninic acid (BCA) by a UV-2100 spectrophotometer (Shimadzu, Japan).[23]

Electron paramagnetic resonance spectroscopy (EPR)

X-band EPR spectra were acquired on a JES-FA200 spectrometer operating at a microwave frequency of 9.03 GHz according to the method of Wang *et al.*[24] The spectra were acquired over a sweep width of 2000 G, modulation amplitude of 10 G, and a temperature of 100 K.

Reduction of disulfide bonds of TS-PDE by small-molecule reductants

2.5 μM as-purified TS-PDE was incubated with 25 mM DTT, 15 mM GSH, 10 mM TCEP, or 20 mM Vc in 20 mM Tris-HCl (pH 7.4) at 37 °C for 60 min. The mixtures were electrophoresed in 5% stacking and 12% resolving SDS-polyacrylamide gels and stained with Coomassie Brilliant Blue R250.

Determination of the number of disulfide bonds

The number of protein disulfide bonds was determined by the reaction of as-purified TS-PDE with DTNB.[25] As-purified TS-PDE (2.5 μM) in 20 mM Tris-HCl (pH 7.4), containing 0.2 M NaCl, was incubated with 1.0 mM DTNB at 25 °C for 90 min under the following conditions: (I) only TS-PDE; (II) with 6 M guanidinium chloride (GdnCl); and (III) with 6 M GdnCl and 10 mM TCEP. The excess TCEP was removed from the reaction mixture by dialysis under nitrogen protection. The A_{412} was monitored to estimate the number of cysteine residues present as protein–TNB mixed disulfide. A standard curve prepared using several

different concentrations of GSH was used in the calculation of the number of cysteine residues. The number of total cysteine residues (n_1) and the number of cysteine residues present as protein–TNB mixed disulfide (n_2) were determined by relative quantification using the standard curve. The number of cysteine residues present as protein–protein disulfide (n_3) was calculated by eqn (2):

$$n_3 = n_1 - n_2 \quad (2)$$

Inhibition of holo-TS-PDE and Zn^{2+}-TS-PDE by small-molecule reductants

0.1 mM NAD^+ was incubated with 2 μM holo-TS-PDE or Zn^{2+}-TS-PDE in 20 mM Tris-HCl (pH 7.4) with increasing concentrations of DTT, GSH, TCEP or Vc at 37 °C for 15 min. The products were analyzed by HPLC. The PDE activities of holo-TS-PDE and Zn^{2+}-TS-PDE were taken as 100% for the inhibition of holo-TS-PDE and Zn^{2+}-TS-PDE, respectively.

Results

Effect of metal ions on the activity of TS-PDE

The effect of 1 mM Cu^{2+}, Zn^{2+}, Mg^{2+}, Mn^{2+}, Ni^{2+}, Co^{2+} or Ca^{2+} on the PDE activities of holo-TS-PDE and apo-TS-PDE have been determined and the results are shown in Fig. 1. Among the tested metal ions, Zn^{2+}, Mg^{2+}, Mn^{2+}, Ni^{2+}, Co^{2+} and Ca^{2+} do not have significant effects on the PDE activity of holo-TS-PDE. In contrast, Cu^{2+} significantly inhibits the PDE activity of holo-TS-PDE. Apo-TS-PDE can acquire 6.3%, 85.9%, 14.4%, 26.2%, 41.0%, 60.4% and 61.4% of the PDE activity in the presence of 1 mM Cu^{2+}, Zn^{2+}, Mg^{2+}, Mn^{2+}, Ni^{2+}, Co^{2+} and Ca^{2+}, respectively. This result indicates that the PDE activity of TS-PDE does not have an absolute requirement for Cu^{2+} and Zn^{2+}. Mg^{2+}, Mn^{2+}, Ni^{2+}, Co^{2+} and Ca^{2+} ions are all effective for its PDE activity.

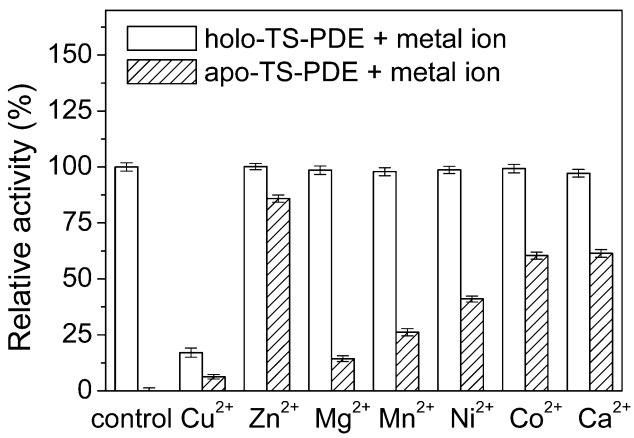

Fig. 1 Effect of various metal ions on the PDE activity of holo-TS-PDE and apo-TS-PDE. 0.1 mM NAD^+ was incubated with 2 μM holo-TS-PDE or apo-TS-PDE in 20 mM Tris-HCl (pH 7.4) in the presence of 1 mM Zn^{2+}, Cu^{2+}, Mg^{2+}, Mn^{2+}, Ni^{2+}, Co^{2+} or Ca^{2+} at 37 °C for 15 min. All products were analyzed by HPLC as described in the Experimental section. The PDE activity of holo-TS-PDE was taken as 100%. Each value represents the mean of three independent determinations.

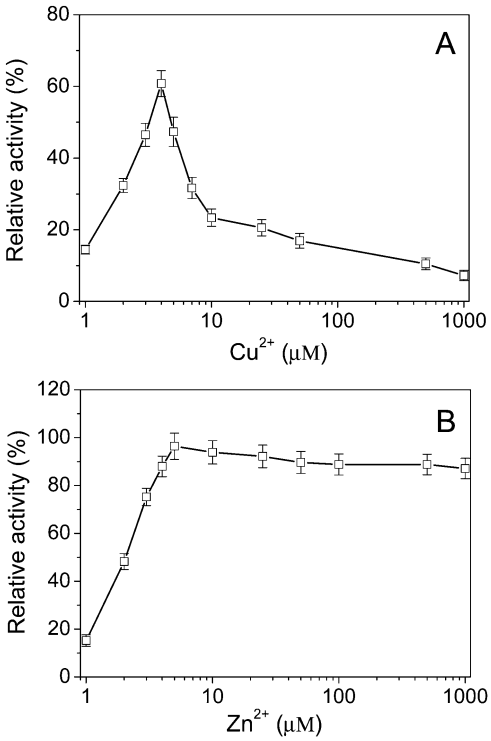

Fig. 2 Activation of the PDE activity of apo-TS-PDE by Cu^{2+} and Zn^{2+}. 0.1 mM NAD^+ was incubated with 2 μM apo-TS-PDE in 20 mM Tris-HCl (pH 7.4) with increasing concentrations of Cu^{2+} (A) or Zn^{2+} (B) at 37 °C for 15 min. All products were analyzed by HPLC as described in the Experimental section. The PDE activity of the holo-TS-PDE was taken as 100%. Each value represents the mean of three independent determinations.

As mentioned previously, Zn^{2+} and Cu^{2+} are present in the native TS-PDE.[19] However, Fig. 1 shows that the PDE activity of holo-TS-PDE is inhibited by 1 mM Cu^{2+} and 1 mM Cu^{2+} restores 6.3% of the activity in apo-TS-PDE. In order to analyze the roles of Cu^{2+} and Zn^{2+} in the PDE activity, the effects of the concentration of Cu^{2+} and Zn^{2+} on the PDE activity of apo-TS-PDE were further determined by HPLC. As shown in Fig. 2A, Cu^{2+} activates the PDE activity of apo-TS-PDE at low concentration ($\leq$4 μM), but significantly inhibits its PDE activity at high concentration (>4 μM) in a concentration-dependent manner. The results suggest that TS-PDE may have two classes of Cu^{2+} binding site, the activator sites and the inhibitor sites. By contrast, although Zn^{2+} also activates the PDE activity of apo-TS-PDE at low concentration ($\leq$5 μM) in a concentration-dependent manner, it does not significantly affect its PDE activity at high concentration (>5 μM) (Fig. 2B), suggesting that TS-PDE only has one class of Zn^{2+}-binding site, *i.e.*, the activator sites.

Analysis of Cu^{2+} and Zn^{2+} binding sites by fluorescence titration

To analyze the Cu^{2+}- and Zn^{2+}-binding sites in TS-PDE and their binding affinities, the fluorescence titration of apo-TS-PDE with Cu^{2+} and Zn^{2+} was performed at an excitation wavelength of 295 nm. Fig. 3(A and C) show the fluorescence spectra of apo-TS-PDE in the presence of various amounts of Cu^{2+} and Zn^{2+}, respectively, which demonstrate a typical fluorescence quenching

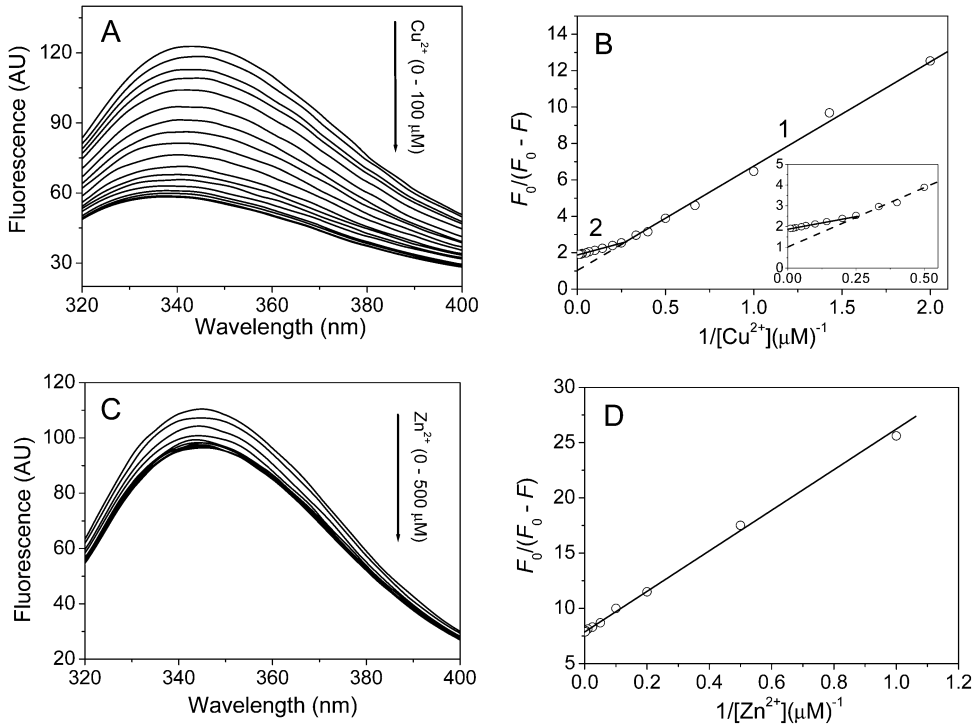

Fig. 3 The fluorescence titration of apo-TS-PDE in 20 mM Tris-HCl (pH 7.4) with Cu^{2+} and Zn^{2+} at 25 °C. (A) The intrinsic fluorescence spectra of apo-TS-PDE with increasing concentrations of Cu^{2+} at an excitation wavelength of 295 nm. (B) Modified Stern–Volmer plots of the fluorescence quenching of apo-TS-PDE by Cu^{2+}. The inset in the figure shows a zoomed view of the 0–0.5 μM^{-1} region. (C) The intrinsic fluorescence spectra of apo-TS-PDE with increasing concentrations of Zn^{2+} at an excitation wavelength of 295 nm. (D) Modified Stern–Volmer plots of the fluorescence quenching of apo-TS-PDE by Zn^{2+}. F_0 and F are the fluorescence intensities of apo-TS-PDE at 344 nm in the absence and presence of metal ion, respectively.

of protein by the two metal ions. Fig. 3(B and D) depict modified Stern–Volmer plots for the quenching of intrinsic fluorescence of apo-TS-PDE by the two metal ions. A linear modified Stern–Volmer plot was observed for the binding of apo-TS-PDE with Zn^{2+}, yielding a f_a of (12.8 ± 0.2)% and a K of $(4.38 \pm 0.07) \times 10^5\ M^{-1}$ (means ± SD, $n = 3$), while the plot for the binding of apo-TS-PDE with Cu^{2+} obviously shows two intersecting straight lines yielding a f_{a1} of (99.6 ± 1.7)% and a K_1 of $(1.59 \pm 0.02) \times 10^5\ M^{-1}$ for line 1 and a f_{a2} of (52.9 ± 0.4)% and a K_2 of $(7.62 \pm 0.08) \times 10^5\ M^{-1}$ (means ± SD, $n = 3$) for line 2. There are one and two apparent association constants for the binding of apo-TS-PDE with Zn^{2+} and Cu^{2+}, respectively, suggesting the presence of one type of Zn^{2+}-binding site and two types of Cu^{2+}-binding site in apo-TS-PDE, respectively.

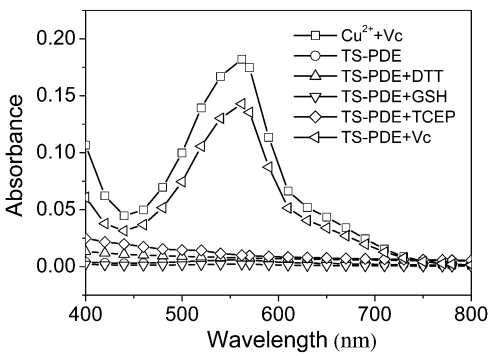

Fig. 4 Reduction of Cu^{2+} in as-purified TS-PDE by DTT, GSH, TCEP and Vc. As-purified TS-PDE (10 μM) was incubated with 25 mM DTT, 15 mM GSH, 10 mM TCEP or 20 mM Vc in 20 mM Tris-HCl (pH 7.4) containing 0.2 M NaCl at 37 °C for 60 min and then the absorbance spectrum of the mixture was recorded after addition of 1 mM BCA. The concentration of free Cu^{2+} ion is 10 μM.

Reduction of Cu^{2+} in as-purified TS-PDE by small-molecule reductants

As mentioned earlier, among all identified PDEs, only TS-PDE contains Cu^{2+}. DTT, GSH, TCEP and Vc have all been reported to reduce Cu^{2+} in Cu^{2+}-containing proteins to Cu^+.[26–28] Therefore, we investigated the effect of reductants on the valence of the copper ion in as-purified TS-PDE. As shown in Fig. 4, free Cu^{2+} ion produces a peak at 560 nm after incubation with 20 mM Vc and 1 mM BCA. This is because Vc reduces Cu^{2+} to Cu^+ and then Cu^+ binds to BCA to form a Cu^+-BCA_2 complex which has a high absorption coefficient at 560 nm.[29] Similarly, an absorbance peak at 560 nm appears after incubation of as-purified TS-PDE with 20 mM Vc and 1 mM BCA, which corresponds to the peak of the Cu^+-BCA_2 complex, revealing that Cu^{2+} in as-purified TS-PDE is reduced to Cu^+ by Vc. However, no peak is observed at 560 nm after incubation of as-purified TS-PDE with other reductants (25 mM DTT, 15 mM GSH or 10 mM TCEP) and 1 mM BCA. It was reported that DTT, GSH and TCEP could all bind with Cu^+ [28,30,31] and the Cu^+-DTT_2 complex had a stability constant higher than that of Cu^+-BCA_2.[32] DTT, GSH and TCEP might also reduce the Cu^{2+} in TS-PDE to Cu^+ and bind with Cu^+, thus blocking the interaction of Cu^+ with BCA.

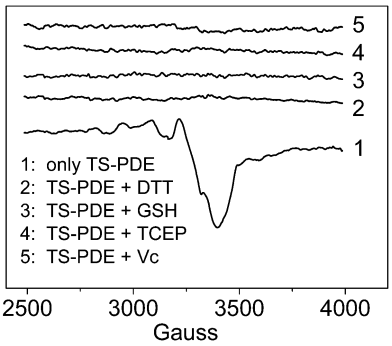

Fig. 5 The effects of reductants on electron paramagnetic resonance spectroscopy (EPR) of as-purified TS-PDE. 150 μM as-purified TS-PDE was incubated with 25 mM DTT (2), 15 mM GSH (3), or 10 mM TCEP (4) or 20 mM Vc (5) in 20 mM Tris-HCl (pH 7.4) containing 0.1 M NaCl and 20% (v/v) dimethylformamide at 37 °C for 60 min and then EPR spectrum of the mixture was recorded at 100 K. The microwave frequency is 9.03 GHz.

The reduction of Cu^{2+} by DTT, GSH, TCEP and Vc was confirmed by using EPR spectroscopy. As shown in Fig. 5, a typical paramagnetic signal of Cu^{2+} is observed for as-purified TS-PDE due to the d^9 electron configuration of Cu^{2+}. The paramagnetic signal of Cu^{2+} disappears after incubation of as-purified TS-PDE with 25 mM DTT, 15 mM GSH, 10 mM TCEP or 20 mM Vc, indicating that paramagnetic Cu^{2+} in as-purified TS-PDE is reduced by DTT, GSH, TCEP or Vc to diamagnetic Cu^{+} with a d^{10} electron configuration.

Reduction of disulfide bonds by small-molecule reductants

The effects of reductants on the disulfide bonds in as-purified TS-PDE were analyzed by SDS-PAGE. As shown in Fig. 6, as-purified TS-PDE gives a single band at 100 kDa (lane 1). After prior incubation with 25 mM DTT, 10 mM TCEP or 15 mM GSH, as-purified TS-PDE gives a single band at about 50 kDa (lanes 3, 4, and 5). This observation reveals that the disulfide bonds between the two chains of the enzyme have been completely cleaved by DTT, TCEP, or GSH. In contrast, after prior incubation with 20 mM Vc, as-purified TS-PDE gives a single band at 100 kDa (lane 6), which is equal to the molecular weight of whole protein, indicating that Vc does not reduce the disulfide bonds between the two chains of the enzyme.

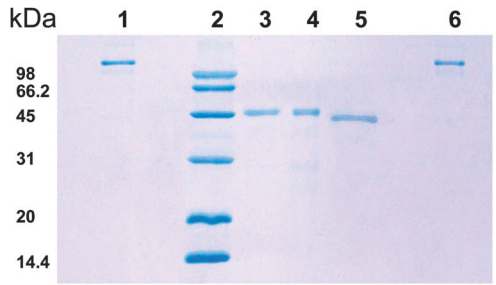

Fig. 6 SDS-polyacrylamide gel electrophoresis of TS-PDE. As-purified TS-PDE was electrophoresed in 12% polyacrylamide gel containing 0.1% SDS under reducing (lanes 2–6) or nonreducing (line 1) conditions. Lane 1: TS-PDE only; lane 2: molecular mass markers; lane 3: TS-PDE + 25 mM DTT; lane 4: TS-PDE + 10 mM TCEP; lane 5: TS-PDE + 15 mM GSH; lane 6: TS-PDE + 20 mM Vc.

To quantitatively analyze small-molecule reductant-induced cleavage of disulfide bonds in as-purified TS-PDE, the enzyme was incubated at 25 °C for 90 min in the absence or presence of each reductant. The number of sulfhydryl groups was estimated by measuring the absorbance value at 412 nm following reaction with 1 mM DTNB. The DTNB absorption value of 0.0821 at 412 nm is equivalent to one sulfhydryl group. Four free cysteine residues have been detected in as-purified TS-PDE, suggesting that these cysteine residues are exposed and accessible to DTNB. After addition of 25 mM DTT, 15 mM GSH or 10 mM TCEP, the absorbance at 412 nm increases from 0.339 ± 0.002 to 0.812 ± 0.005, 0.654 ± 0.05 or 0.817 ± 0.007 (means ± SD, n = 3), indicating that the number of sulfhydryl groups in the protein increases from 4 to 10, 8, or 10. The total number of free cysteine residues in the protein after unfolding by 6 M GdnCl has been determined to be 10 and 24 in the absence and presence of 10 mM TCEP, respectively, indicating that each as-purified TS-PDE molecule contains seven disulfide bonds. GdnCl-induced unfolding of as-purified TS-PDE results in an increase in the number of free cysteine residues from 4 to 10, which demonstrates that six free cysteine residues are buried in the folded protein. Incubation of as-purified TS-PDE with another reductant, Vc (20 mM), results in a slight change in the absorbance value at 412 nm from 0.339 ± 0.002 to 0.347 ± 0.005 (means ± SD, n = 3). This small difference is within the experimental error, suggesting that the number of sulfhydryl groups in the protein is not affected by Vc. This observation is consistent with the result from SDS-PAGE.

Inhibition of holo-TS-PDE and Zn^{2+}-TS-PDE by small-molecule reductants

To examine whether the disulfide bonds and Cu^{2+} in holo-TS-PDE are required for its PDE activity, we have investigated the inhibition of the PDE activity of holo-TS-PDE by small-molecule reductants. As shown in Fig. 7, DTT, GSH, TCEP and Vc inhibit the PDE activity of holo-TS-PDE in a concentration-dependent manner. The values of the half maximal inhibitory concentrations (IC_{50}) were obtained based on the data from Fig. 7. As shown in Table 1, the calculated IC_{50} values are 6.90 ± 0.06 mM, 2.56 ± 0.04 mM, 1.48 ± 0.03 mM and 2.87 ± 0.04 mM (means ± SD, n = 3) for DTT, GSH, TCEP and Vc, respectively, indicating that their inhibition efficiencies follow the trend: TCEP > GSH > Vc > DTT.

DTT, GSH and TCEP can reduce both Cu^{2+} and disulfide bonds in as-purified TS-PDE. To determine whether disulfide bonds are essential for the PDE activity of TS-PDE, we have investigated the inhibition of the PDE activity of Zn^{2+}-TS-PDE by small-molecule reductants. All DTT, GSH and TCEP inhibit the PDE activity of Zn^{2+}-TS-PDE in a concentration-dependent manner. The calculated IC_{50} value are 8.62 ± 0.09 mM, 3.45 ± 0.03 mM and 1.84 ± 0.03 mM (means ± SD, n = 3) for DTT, GSH and TCEP (Table 1), respectively, indicating that their inhibition efficiencies follow the trend: TCEP > GSH > DTT. However, Vc does not inhibit the PDE activity of Zn^{2+}-TS-PDE up to a concentration of 20 mM.

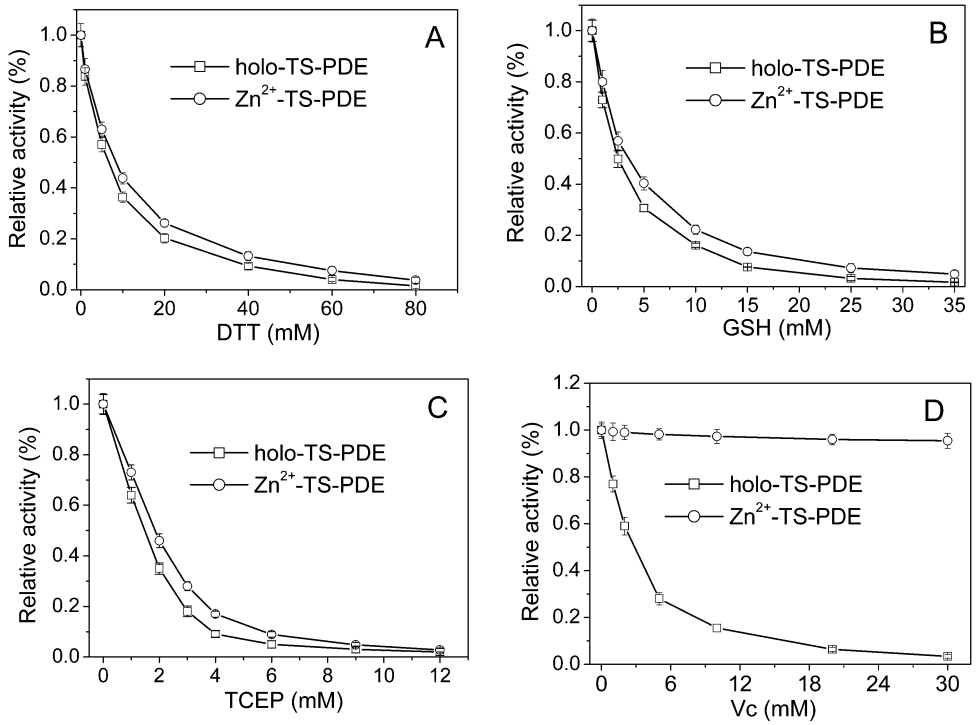

Fig. 7 Inhibition of PDE activities of holo-TS-PDE and Zn^{2+}-TS-PDE by DTT, GSH, TCEP, and Vc. 0.1 mM NAD^+ was incubated with 2 μM holo-TS-PDE or Zn^{2+}-TS-PDE in 20 mM Tris-HCl (pH 7.4) at 37 °C for 15 min with increasing concentrations of DTT (A), GSH (B), TCEP (C), or Vc (D). All products were analyzed by HPLC as described in the Experimental section. The PDE activity of holo-TS-PDE and Zn^{2+}-TS-PDE were taken as 100% for the inhibitions of holo-TS-PDE and Zn^{2+}-TS-PDE, respectively. Each value represents the mean of three independent determinations.

Table 1 IC_{50} values of reductants for holo-TS-PDE and Zn^{2+}-TS-PDE and redox potentials of reductants. The IC_{50} values are mean ± SD of $n = 3$

Reductants	IC_{50} for holo-TS-PDE (mM)	IC_{50} for Zn^{2+}-TS-PDE (mM)	Redox potential (V)
TCEP	1.48 ± 0.03	1.84 ± 0.03	−0.29
GSH	2.56 ± 0.04	3.45 ± 0.03	−0.16
Vc	2.87 ± 0.04	—	−0.127
DTT	6.90 ± 0.06	8.62 ± 0.09	−0.33

Discussion

TS-PDE is different from other PDEs, since it consists of two different chains linked with disulfide bond(s) and contains both Cu^{2+} and Zn^{2+}.[19] DTT, GSH and TCEP can reduce Cu^{2+} in as-purified TS-PDE and the disulfide bonds between its two chains as determined by EPR spectroscopy and SDS-PAGE (Fig. 5 and 6), which results in inhibition of its PDE activity. Vc reduces Cu^{2+} in the as-purified TS-PDE to Cu^+, as evidenced by the formation of the Cu^+-BCA_2 complex (Fig. 4) and the disappearance of the paramagnetic signal of Cu^{2+} (Fig. 5), but it can not reduce disulfide bonds between the two chains of TS-PDE (Fig. 6). The reduction of Cu^{2+} to Cu^+ by Vc results in the inhibition of the PDE activity of the enzyme. These observations indicate that Cu^{2+} is the activator of TS-PDE. By contrast, Cu^+ can not stimulate its PDE activity.

The fluorescence titration data demonstrate that TS-PDE has two classes of Cu^{2+}-binding site (Fig. 3). Fig. 2A shows that Cu^{2+} activates the PDE activity of apo-TS-PDE at low concentration, but significantly inhibits its PDE activity at high concentration, suggesting that the Cu^{2+} ions as activators may bind in the catalytic site with high binding affinity, while the Cu^{2+} ions as inhibitors may bind in low-affinity sites. Valério *et al.* also found that Cu^{2+} at high concentration (>1 mM) significantly inhibited the activity of PDE from *Bothrops alternatus* snake venom.[9] Cu^{2+}-induced significant fluorescence quenching of TS-PDE with an obvious blue-shift of the maximum emission from 344 nm to 338 nm suggests that (1) a dramatic conformational change of TS-PDE is induced upon Cu^{2+} binding to the low-affinity sites; (2) this conformational change may affect the microenvironment of the catalytic site or mask the catalytic site which results in the inhibition of the enzyme. Hoffmann *et al.*[33] reported that the substrate NAD^+ can bind with Cu^{2+}. TS-PDE may not be able to hydrolyze the complex of Cu^{2+}-NAD^+, which may be another explanation for the inhibition of the PDE activity of the enzyme by the Cu^{2+} ions. Although we cannot infer the actual mechanism of the activation and inhibition by Cu^{2+} ions from the present data, it is certain that Cu^{2+} ions function as a switch for the PDE activity of TS-PDE. Further investigation is necessary to elucidate the mechanism of the activation and inhibition by Cu^{2+} ions.

In contrast to Cu^{2+} binding sites, there is only one class of Zn^{2+}-binding site in TS-PDE as determined by fluorescence titration (Fig. 3). Zn^{2+} activates the PDE activity of apo-TS-PDE at low concentration, and does not inhibit its PDE activity at high concentration (Fig. 2B), suggesting that the Zn^{2+} ions only act as activators and may bind in the catalytic site with high

binding affinity. Mg^{2+}, Mn^{2+}, Ni^{2+}, Co^{2+} and Ca^{2+} have no obvious effects on the PDE activity of holo-TS-PDE (Fig. 1), revealing that these metal ions are not inhibitors of the enzyme. The PDE activity of apo-TS-PDE is partially recovered by Mg^{2+}, Mn^{2+}, Ni^{2+}, Co^{2+} and Ca^{2+}, indicating that these metal ions are all effective for its PDE activity. The mechanism of activation of TS-PDE by these metal ions has not been studied in detail and could be a subject for further investigation.

As shown in Fig. 2, apo-TS-PDE (2 μM) exhibits the maximum PDE activity in the presence of 4 μM Cu^{2+}, suggesting that TS-PDE has two high-affinity Cu^{2+}-binding sites. Fig. 3B shows that the two straight lines cross at 4 μM Cu^{2+}, suggesting that 2 μM apo-TS-PDE can bind with 4 μM Cu^{2+} in the high-affinity sites. These results taken together indicate that TS-PDE has two high-affinity Cu^{2+}-binding sites.

Previous studies show that as-purified TS-PDE probably has a bimetallic cluster (Cu^{2+}–Zn^{2+}) in its hydrolysis center.[19] Vc does not reduce the disulfide bonds (Fig. 6) and Zn^{2+}, but it can reduce Cu^{2+} to Cu^{+}, as evidenced by the formation of the Cu^{+}-BCA_2 complex (Fig. 4). The reduction of Cu^{2+} results in the loss of the PDE activities of holo-TS-PDE (Fig. 7D), indicating that although one Zn^{2+} is still in its hydrolysis center, the enzyme loses almost all PDE activity after reduction of Cu^{2+} by Vc. Therefore, the bimetallic Cu^{2+}–Zn^{2+} hydrolysis center is critical for its PDE activity. Apo-TS-PDE can acquire 96.4% or 60.8% of the PDE activity in the presence of 5 μM Zn^{2+} or 4 μM Cu^{2+} (Fig. 2), suggesting that the Zn^{2+}–Zn^{2+} or Cu^{2+}–Cu^{2+} hydrolysis center is also effective for its PDE activity.

TS-PDE is rich in cysteines. The total number of cysteine residues in as-purified TS-PDE is 24. The number of free cysteine residues detected in as-purified TS-PDE increases from 4 to 10, 8 or 10 after interaction of as-purified TS-PDE with 25 mM DTT, 15 mM GSH or 10 mM TCEP, indicating that three disulfide bonds have been reduced by DTT or TCEP and two disulfide bonds have been reduced by GSH, which may be the reason why GSH-reduced TS-PDE runs faster than DTT- or TCEP-reduced TS-PDE in SDS-PAGE gel (Fig. 6). These results also suggest that the three exposed disulfide bonds are located between the two chains and/or on the surface of the protein. The disulfide bonds between the two chains of the protein can be completely cleaved by DTT, TCEP, or GSH. Although DTT, GSH and TCEP cannot reduce Zn^{2+}, they are able to inhibit the PDE activity of Zn^{2+}-TS-PDE (Fig. 7). These findings agree with data for PDE from *Walterinnesia aegyptia*, the activity of which is inhibited by GSH.[10] The reduction of disulfide bonds is simultaneous with the inhibition of Zn^{2+}-TS-PDE, suggesting that at least one of the three exposed disulfide bonds is critical for the PDE activity of TS-PDE. Interestingly, the IC_{50} value of Zn^{2+}-TS-PDE is greater than that of as-purified TS-PDE for each reductant (DTT, TCEP, or GSH) (Fig. 7), suggesting that the three reductants inhibit the PDE activity through the reduction of both Cu^{2+} and disulfide bonds in as-purified TS-PDE.

Comparison of the IC_{50} values of holo-TS-PDE and Zn^{2+}-TS-PDE with the redox potentials of each reductant[34–37] shows that the inhibition efficiency of the reductant increases with the decrease of its redox potential, except that DTT with the lowest redox potential has the lowest inhibition efficiency (Table 1). The possible reasons may be that these reductants have different redox potentials under the present conditions (pH 7.4, 37 °C) compared with their reported redox potentials at pH 7.0 and DTT, GSH and TCEP can bind with Cu^{+},[28,30,31] which may affect the reduction of Cu^{2+} to Cu^{+} by these reductants. Further investigation is necessary to clarify this issue. TCEP, among the three reductants, has the lowest IC_{50}, due to the fact that TCEP is the most stable and most effective reductant for disulfide bonds.[38,39]

Vc and GSH are biologically-relevant reductants. In living organisms, Vc, as an antioxidant, protects the body against oxidative stress.[40] GSH, as a cellular reductant, reduces disulfide bonds in proteins by acting as an electron donor. The IC_{50} value of GSH is 2.56 ± 0.04 mM for holo-TS-PDE, which is within the range (0.5–10 mM) of GSH concentrations found in eukaryotic cells.[41] Therefore the intracellular concentration of GSH is adequate to affect the PDE activity of TS-PDE.

Conclusion

The present study reveals that TS-PDE has one class of Zn^{2+} binding site and two classes of Cu^{2+} binding site, including the high affinity activator sites and the low affinity sites. Cu^{2+} ions function as a switch for its PDE activity. Vc inhibits the PDE activity of holo-TS-PDE through reduction of the Cu^{2+}, while other reductants, DTT, GSH and TCEP, inhibit the PDE activity of holo-TS-PDE by reducing both the Cu^{2+} and the disulfide bonds. The catalytic activity of TS-PDE relies on the disulfide bonds and the bimetallic cluster.

Acknowledgements

This work was supported by grants from the National Natural Science Foundation of China (Grant No. 21171157, 20871111, 20571069). We thank two reviewers for their constructive comments, which helped improve the quality of this paper.

References

1 Y. H. Jeon, Y. S. Heo, C. M. Kim, Y. L. Hyun, T. G. Lee, S. Ro and J. M. Cho, *Cell. Mol. Life Sci.*, 2005, **62**, 1198–1220.
2 M. Segovia and F. L. Figueroa, *Plant Biosyst.*, 2007, **141**, 123–127.
3 B. L. Dhananjaya and C. J. M. D'souza, *Biochemistry (Moscow)*, 2010, **75**, 1–6.
4 A. Castro, M. J. Jerez, C. Gil and A. Martinez, *Med. Res. Rev.*, 2005, **25**, 229–244.
5 C. Burnouf and M. P. Pruniaux, *Curr. Pharm. Des.*, 2002, **8**, 1255–1296.
6 S. Uckert, P. Hedlund, K. E. Andersson, M. C. Truss, U. Jonas and C. G. Stief, *Eur. Urol.*, 2006, **50**, 1194–1207.
7 C. L. Miller and C. Yan, *J. Cardiovasc. Transl. Res.*, 2010, **3**, 507–515.
8 A. T. Bender and J. A. Beavo, *Pharmacol. Rev.*, 2006, **58**, 488–520.

9 A. A. Valério, A. C. Corradini, P. C. Panunto, S. M. Mello and S. Hyslop, *J. Protein Chem.*, 2002, **21**, 495–503.
10 S. S. Al-Saleh and S. Khan, *Prep. Biochem. Biotechnol.*, 2011, **41**, 262–277.
11 N. Mori, T. Nikai and H. Sugihara, *Int. J. Biochem.*, 1987, **19**, 115–119.
12 S. P. Liu, M. N. Mansour, K. S. Dillman, J. R. Perez, D. E. Danley, P. A. Aeed, S. P. Simons, P. K. LeMotte and F. S. Menniti, *Proc. Natl. Acad. Sci. U. S. A.*, 2008, **105**, 13309–13314.
13 J. Pandit, M. D. Forman, K. F. Fennell, K. S. Dillman and F. S. Menniti, *Proc. Natl. Acad. Sci. U. S. A.*, 2009, **106**, 18225–18230.
14 S. F. Chen, A. F. Yakunin, E. Kuznetsova, D. Busso, R. Pufan, M. Proudfoot, R. Kim and S. H. Kim, *J. Biol. Chem.*, 2004, **279**, 31854–31862.
15 F. Pintus, D. Spano, A. Bellelli, F. Angelucci, G. Floris and R. Medda, *Plant Sci.*, 2009, **177**, 636–642.
16 M. Podobnik, R. Tyagi, N. Matange, U. Dermol, A. K. Gupta, R. Mattoo, K. Seshadri and S. S. Visweswariah, *J. Biol. Chem.*, 2009, **284**, 32846–32857.
17 L. Hamza, C. Gargioli, S. Castelli, S. Rufini and F. Laraba-Djebari, *Biochimie*, 2010, **92**, 797–805.
18 R. B. Zingali, *Toxin Rev.*, 2007, **26**, 25–46.
19 L. Peng, X. Xu, D. Shen, Y. Zhang, J. Song, X. Yan and M. Guo, *Biochimie*, 2011, **93**, 1601–1609.
20 C. V. Kumar and M. R. Duff, Jr., *Photochem. Photobiol. Sci.*, 2008, **7**, 1522–1530.
21 S. S. Lehrer, *Biochemistry*, 1971, **10**, 3254–3263.
22 X. Xu, L. Zhang, Z. Luo, D. Shen, H. Wu, L. Peng, J. Song and Y. Zhang, *Metallomics*, 2010, **2**, 480–489.
23 L. A. Yatsunyk and A. C. Rosenzweig, *J. Biol. Chem.*, 2007, **282**, 8622–8631.
24 H. Wang, F. Zhong, J. Pan, W. Li, J. Su, Z. X. Huang and X. Tan, *JBIC, J. Biol. Inorg. Chem.*, 2012, **17**, 719–730.
25 O. W. Griffith, *Anal. Biochem.*, 1980, **106**, 207–212.
26 J. C. Dumville and S. C. Fry, *Planta*, 2003, **217**, 951–961.
27 M. Valko, C. J. Rhodes, J. Moncol, M. Izakovic and M. Mazur, *Chem.-Biol. Interact.*, 2006, **160**, 1–40.
28 P. A. Thibodeau, S. Kocsis-Bedard, J. Courteau, T. Niyonsenga and B. Paquette, *Free Radical Biol. Med.*, 2001, **30**, 62–73.
29 T. Huang, M. Long and B. Huo, *Open Biomed. Eng. J.*, 2010, **4**, 271–278.
30 A. Krezel, W. Lesniak, M. Jezowska-Bojczuk, P. Mlynarz, J. Brasun, H. Kozlowski and W. Bal, *J. Inorg. Biochem.*, 2001, **84**, 77–88.
31 A. Urvoas, M. Moutiez, C. Estienne, J. Couprie, E. Mintz and L. Le Clainche, *Eur. J. Biochem.*, 2004, **271**, 993–1003.
32 R. Miras, I. Morin, O. Jacquin, M. Cuillel, F. Guillain and E. Mintz, *JBIC, J. Biol. Inorg. Chem.*, 2008, **13**, 195–205.
33 S. K. Hoffmann, J. Goslar, S. Lijewski, K. Basinski, A. Gasowska and L. Lomozik, *J. Inorg. Biochem.*, 2012, **111**, 18–24.
34 P. K. Pullela, T. Chiku, M. J. C. Iii and D. S. Sem, *Anal. Biochem.*, 2006, **352**, 265–273.
35 L. W. Mapson and F. A. Isherwood, *Biochem. J.*, 1963, **86**, 173–191.
36 H. Borsook and G. Keighley, *Proc. Natl. Acad. Sci. U. S. A.*, 1933, **19**, 875–878.
37 W. W. Cleland, *Biochemistry*, 1964, **3**, 480–482.
38 U. T. Rüegg, J. Rudinger, C. H. W. Hirs and N. T. Serge, *Methods in enzymology*, Academic Press, 1977, vol. 47, pp. 111–116.
39 T. L. Kirley, *Anal. Biochem.*, 1989, **180**, 231–236.
40 S. J. Padayatty, A. Katz, Y. Wang, P. Eck, O. Kwon, J.-H. Lee, S. Chen, C. Corpe, A. Dutta, S. K. Dutta and M. Levine, *J. Am. Coll. Nutrition*, 2003, **22**, 18–35.
41 A. Meister and M. E. Anderson, *Annu. Rev. Biochem.*, 1983, **52**, 711–760.